© 2014. Published by The Company of Biologists Ltd | Development (2014) 141, 2712-2723 doi:10.1242/dev.107508

RESEARCH ARTICLE

Clathrin regulates centrosome positioning by promoting acto-myosin cortical tension in *C. elegans* embryos

Zoltán Spiró, Kalyani Thyagarajan, Alessandro De Simone, Sylvain Träger, Katayoun Afshar and Pierre Gönczy*

ABSTRACT

Regulation of centrosome and spindle positioning is crucial for spatial cell division control. The one-cell *Caenorhabditis elegans* embryo has proven attractive for dissecting the mechanisms underlying centrosome and spindle positioning in a metazoan organism. Previous work revealed that these processes rely on an evolutionarily conserved force generator complex located at the cell cortex. This complex anchors the motor protein dynein, thus allowing cortical pulling forces to be exerted on astral microtubules emanating from microtubule organizing centers (MTOCs). Here, we report that the clathrin heavy chain CHC-1 negatively regulates pulling forces acting on centrosomes during interphase and on spindle poles during mitosis in one-cell *C. elegans* embryos. We establish a similar role for the cytokinesis/apoptosis/RNA-binding protein CAR-1 and uncover that CAR-1 is needed to maintain proper levels of CHC-1. We demonstrate that CHC-1 is necessary for normal organization of the cortical acto-myosin network and for full cortical tension. Furthermore, we establish that the centrosome positioning phenotype of embryos depleted of CHC-1 is alleviated by stabilizing the acto-myosin network. Conversely, we demonstrate that slight perturbations of the acto-myosin network in otherwise wild-type embryos results in excess centrosome movements resembling those in *chc-1*(*RNAi*) embryos. We developed a 2D computational model to simulate cortical rigidity-dependent pulling forces, which recapitulates the experimental data and further demonstrates that excess centrosome movements are produced at medium cortical rigidity values. Overall, our findings lead us to propose that clathrin plays a critical role in centrosome positioning by promoting acto-myosin cortical tension.

KEY WORDS: Centrosome positioning, Clathrin heavy chain, Cortical tension

INTRODUCTION

Asymmetric cell division is important for generating cell diversity during development and in stem cell lineages, notably by ensuring the proper segregation of cell fate determinants (reviewed by Gönczy, 2008; Knoblich, 2008; Noatynska and Gotta, 2012). Spindle positioning is paramount for successful asymmetric cell division. In animal cells, the location of centrosomes before mitosis and of spindle poles during mitosis [centrosomes and spindle poles are referred to collectively hereafter as microtubule organizing centers (MTOCs)] together determine spindle position because the cleavage furrow bisects the spindle at the end of mitosis. Therefore, MTOC positioning dictates the relative size and position of daughter cells. Despite significant advances in recent years, the mechanisms governing MTOC positioning in the context of the organism remain incompletely understood.

The one-cell embryo of *C. elegans* has emerged as an attractive model to dissect the mechanisms underlying MTOC positioning, which can be observed with high spatial and temporal resolution using time-lapse differential interference contrast (DIC) microscopy (reviewed by Oegema and Hyman, 2006). Soon after fertilization, local relaxation of the cortical acto-myosin cortex at the presumptive posterior pole initiates a cascade of events that results in the establishment of anteroposterior (AP) embryonic polarity (reviewed by Gönczy and Rose, 2005). Soon after polarity establishment and meeting of the two pronuclei in the posterior embryo half, a series of stereotypical MTOC positioning events take place. First, during prophase, the two centrosomes and associated pronuclei move smoothly towards the cell center while undergoing a 90° rotation. This process is referred to collectively as centration/rotation and positions the centrosomes in the middle of the embryo and along the AP axis before nuclear envelope breakdown (NEBD) (see supplementary material Movie 1). Second, following spindle assembly, the metaphase spindle is displaced towards the embryo posterior. Posterior displacement becomes more pronounced in anaphase, when it is accompanied by transverse oscillations of the posterior spindle pole. As a result of posterior spindle displacement, the cleavage furrow parts the zygote into a larger anterior blastomere and a smaller posterior one.

MTOC positioning in the one-cell *C. elegans* embryo relies on an evolutionarily conserved ternary complex located at the cell cortex that is necessary to generate pulling force on astral microtubules (reviewed by Kotak and Gönczy, 2013). In worms, this ternary complex comprises the partially redundant Gα subunits of heterotrimeric G proteins GOA-1 and GPA-16, the GoLoco motif containing proteins GPR-1/2, as well as the coil-coiled protein LIN-5 (Gotta and Ahringer, 2001; Colombo et al., 2003; Gotta et al., 2003; Srinivasan et al., 2003). The ternary complex anchors the minus-end directed motor dynein at the cell cortex, leading to the generation of pulling forces on astral microtubules emanating from centrosomes and spindle poles (Kozlowski et al., 2007; Nguyen-Ngoc et al., 2007; Laan et al., 2012; Rai et al., 2013). Force generation is thought to be exerted by dynein motor activity per se or by the ability of dynein to maintain association with force-generating depolymerizing microtubules (Couwenbergs et al., 2007; Nguyen-Ngoc et al., 2007). Slightly more GPR-1/2 is present on the anterior cortex during centration/rotation (Laan et al., 2012; Panbianco et al., 2008; Park and Rose, 2008; Rai et al., 2013), probably explaining the anterior-directed movement of centrosomes during that stage. Conversely, slightly more GPR-1/2 is found on the posterior cortex during anaphase (Colombo et al., 2003; Gotta et al., 2003; Tsou et al., 2003), probably explaining the imbalance of net pulling forces exerted on the two spindle poles at that stage.

Swiss Institute for Experimental Cancer Research (ISREC), School of Life Sciences, Swiss Federal Institute of Technology (EPFL) Lausanne, Lausanne CH-1015, Switzerland.

*Author for correspondence (pierre.gonczy@epfl.ch)

Received 23 December 2013; Accepted 12 May 2014

Development (2014) 141, 2712-2723 doi:10.1242/dev.107508

Whereas the ternary complex and dynein are at the core of the force generation machinery, it is clear that further regulation can modulate force generation. For instance, the PP6 phosphatase PPH-6 and its partner SAPS-1 are positive regulators of force generation that ensure proper levels of cortical GPR-1/2 (Afshar et al., 2010). Conversely, the Gβγ proteins GPB-1 and GPC-2 act as negative regulators by competing with GPR-1/2 for binding to the Gα proteins (Tsou et al., 2003; Afshar et al., 2004). Another example of negative regulation is offered by the casein kinase CSNK-1, which normally limits GPR-1/2 cortical levels (Panbianco et al., 2008). Spatial regulation is also important. Thus, the DEP domain protein LET-99 is present in a posterior-lateral band, where it prevents accumulation of cortical GPR-1/2 (Tsou et al., 2003; Krueger et al., 2010). More general cellular processes are also harnessed to modulate forces pulling on centrosomes and spindle poles. Thus, endosomal trafficking of GPB-1 occurs in a cell-cycle-regulated manner, and it has been proposed that trafficking-dependent downregulation of cortical GPB-1 during mitosis is important to allow association of GPR-1/2 with the Gα proteins (Thyagarajan et al., 2011). Moreover, interfering with the actin cytoskeleton during mitosis results in increased pulling forces on the anterior side (Afshar et al., 2010; Berends et al., 2013), although whether this occurs via an impact on ternary complex components, and whether a similar relationship pertains to centration/rotation are unanswered questions.

RESULTS

The clathrin heavy chain CHC-1 negatively regulates pulling forces in *C. elegans* embryos

In the course of an RNAi-based functional genomic screen (Gönczy et al., 2000), it was found that depletion of the clathrin heavy chain CHC-1 results in several phenotypes visible by DIC in one-cell embryos, which we set out to further investigate. As in other systems, clathrin plays a role in receptor-mediated endocytosis in *C. elegans* and is thus required for proper yolk intake in the oocyte (Fig. 1A,B, insets) (Grant and Hirsh, 1999). We found in addition that *chc-1*(*RNAi*) one-cell embryos exhibit stereotyped MTOC positioning defects that are detailed below.

During centration/rotation, instead of the smooth movement of centrosomes and associated pronuclei towards the anterior that are characteristic of the wild-type, excess back and forth movements are observed in *chc-1*(*RNAi*) embryos (compare Fig. 1A with 1B, as well as Fig. 1C with 1D; supplementary material Movies 1 and 2). To quantify this phenotype, we determined the velocity of the movements of centrosomes as well as their angular displacement during centration/rotation (see supplementary material Fig. S1A for a schematic of the quantification methods). We found that both metrics are significantly higher in *chc-1*(*RNAi*) embryos than in the wild type (Fig. 1E,F).

The net pulling force acting on spindle poles during anaphase can be estimated using laser microbeam-mediated severing of astral microtubules (Grill et al., 2001). We designed an analogous assay during centration/rotation, performing severing of astral microtubules emanating from the anterior or the posterior centrosome. The extent of anteriorly directed net pulling forces was inferred from the velocity of anteriorly directed movements following posterior severing, and that of posteriorly directed net pulling forces from the velocity of posteriorly directed movements following anterior severing (see supplementary material Fig. S1B for a schematic of these experiments). The resulting analysis revealed that net forces are larger on the anterior than on the posterior at this stage, in line with analogous experiments in which centrosomes were targeted instead with a laser microbeam (Labbe et al., 2004). Moreover, we found that peak velocities following an anterior cut are lower in *gpr-1/2*(*RNAi*) embryos than in the wild type (supplementary material Fig. S1C), as anticipated from the ternary complex playing a role in centration/rotation (Park and Rose, 2008). Most importantly, these experiments revealed also that net pulling forces are substantially higher both on the anterior and posterior centrosomes in *chc-1*(*RNAi*) compared with the wild type (Fig. 1G). This increase is not due merely to the depletion of yolk granules, as peak velocities after an anterior cut are indistinguishable from the wild type in *rme-2*(*RNAi*) embryos (supplementary material Fig. S1C), in which yolk granules are also sparse due to defective endocytosis (Grant and Hirsh, 1999). We also observed that even though centrosomes in *chc-1*(*RNAi*) embryos occupy a normal position by the end of centration, they are displaced prematurely towards the posterior by the time of NEBD, suggestive of higher posterior pulling forces (Fig. 1M; supplementary material Movies 1 and 2). Nevertheless, the spindle is oriented along the AP axis in *chc-1*(*RNAi*) embryos as it is in the wild type (supplementary material Fig. S1F,G).

An MTOC positioning phenotype was also observed thereafter in *chc-1*(*RNAi*) embryos. Indeed, we found that the anterior spindle pole of *chc-1*(*RNAi*) embryos exhibits excess oscillations during anaphase (Fig. 1, compare H with I, as well as J with K; supplementary material Movies 1 and 2), suggestive of increased net forces pulling on the anterior spindle pole. To test whether this is the case, we performed spindle-severing experiments during anaphase (Grill et al., 2001). We found that the average peak velocity of the liberated anterior spindle pole is higher indeed in *chc-1*(*RNAi*) embryos than in the wild type (Fig. 1L). Despite such alterations in net pulling forces, the final position of the anaphase spindle and thus the placement of the cleavage furrow are essentially unchanged in *chc-1*(*RNAi*) embryos, presumably because of the above-mentioned premature posterior displacement of centrosomes at the time of NEBD (Fig. 1M).

Overall, we conclude that the clathrin heavy chain negatively regulates pulling forces on the anterior side during centration/rotation and anaphase in *C. elegans* embryos.

CAR-1 depletion also leads to MTOC positioning defects and results in lower CHC-1 levels

We were intrigued by the fact that embryos depleted of CAR-1 exhibit MTOC positioning phenotypes that appeared reminiscent of those in *chc-1*(*RNAi*) embryos (Squirrell et al., 2006). CAR-1 is a multifunctional RNA-binding protein that plays a role in germline apoptosis (Boag et al., 2005), in regulating P-granule-related mRNAs (Noble et al., 2008) and in cytokinesis (Audhya et al., 2005). Intriguingly, overexpression of the CAR-1 homolog Scd6p/Lsm13p in budding yeast suppresses clathrin deficiency (Nelson and Lemmon, 1993). Although several aspects of CAR-1 function have been characterized previously in *C. elegans*, we focused on the fact that CAR-1 depletion leads to excess back and forth movements of centrosomes during centration/rotation, resulting in increased centrosome movements and angular displacement during centration/rotation compared with the wild type (Fig. 2A-F; supplementary material Movie 3). Moreover, we found that the anterior spindle pole undergoes excess oscillations during mitosis in *car-1*(*RNAi*) embryos (Fig. 2G-J; supplementary material Movie 3). These phenotypic manifestations are similar to the ones in *chc-1*(*RNAi*) embryos (Fig. 2A-J, compare with Fig. 1). Therefore, we examined the distribution of clathrin in *car-1*(*RNAi*) embryos. In control one-cell embryos, GFP-CHC-1 is present primarily in the cytoplasm, is enriched on the spindle and is also detectable in the vicinity of the cortex (Fig. 2K). Strikingly, we found that the overall levels of

Development (2014) 141, 2712-2723 doi:10.1242/dev.107508

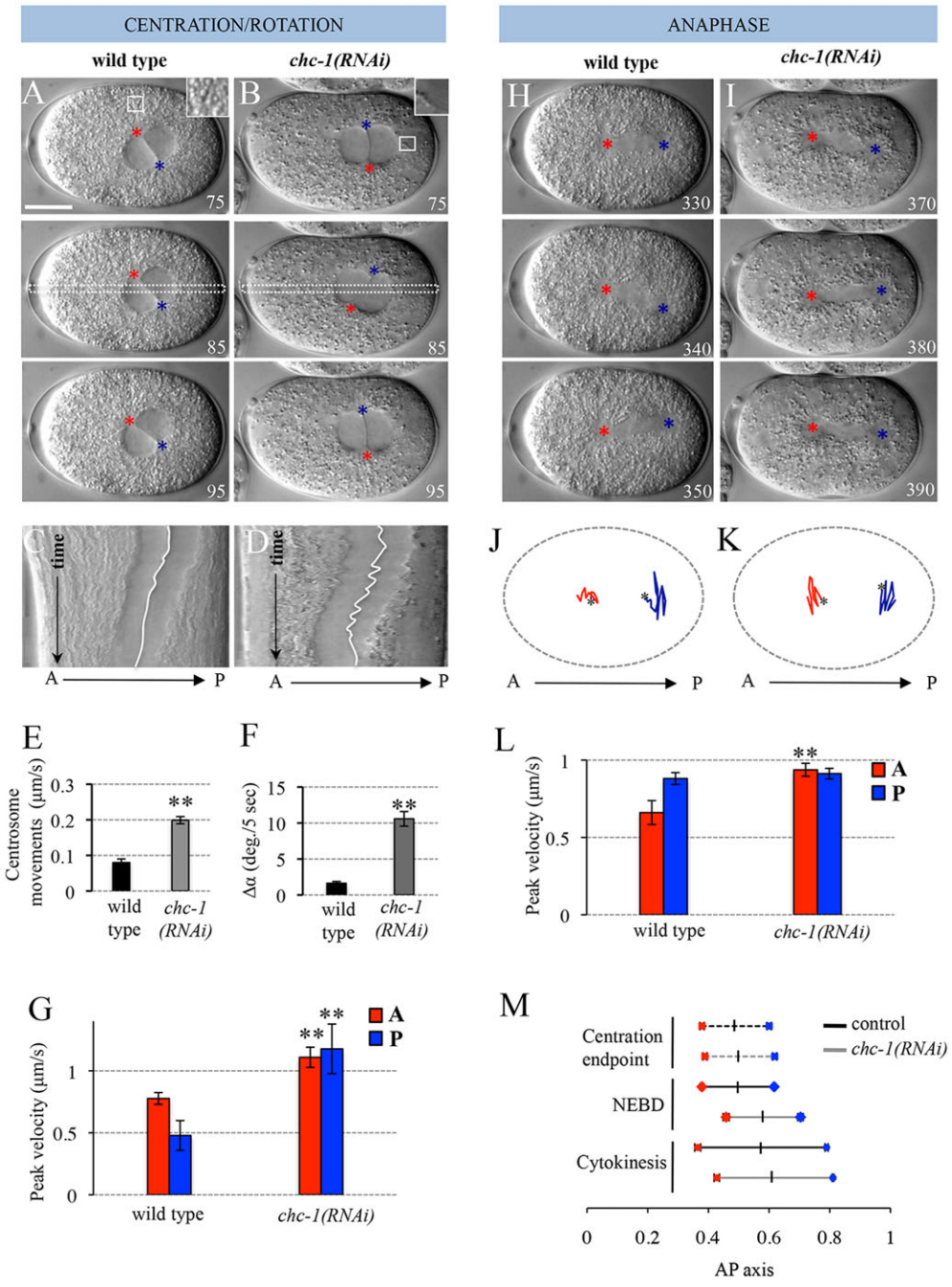

Fig. 1. Clathrin negatively regulates net pulling forces acting on centrosomes during centration/rotation and on spindle poles during anaphase. (A-G) Centration/rotation. (A,B) Centrosome position in wild-type (A) and *chc-1*(*RNAi*) (B) embryos monitored by time-lapse DIC microscopy. Centrosomes are marked with red and blue asterisks. Insets illustrate the depletion of yolk granules in *chc-1*(*RNAi*) embryos. Here and in other figures, time is indicated in seconds, with *t*=0 corresponding to pronuclear meeting unless stated otherwise, and scale bars represent 10 µm. See also supplementary material Movies 1 and 2. (C,D) Kymographs of the areas marked by dashed white rectangles in A and B. The white line delineates the position of the nuclear envelopes of the joined pronuclei. The embryos were imaged with a frame rate of 0.5 s to acquire a kymograph with high resolution. Here and in the following cases, we used the first 150 s from pronuclear meeting onwards to compose the kymographs. (E,F) Average centrosome movements (E) and average angular displacement (F) in wild-type and *chc-1*(*RNAi*) embryos. See also supplementary material Fig. S1A. *n*=10 embryos from three experiments in every case. Here and in all figures, error bars represent the s.e.m. and the statistical significance was calculated using unpaired Student's *t*-test; significance levels are **P*<0.05, ***P*<0.01. (G) Average peak velocities of centrosomes following laser severing of microtubules during centration rotation. Posterior cuts (red) and anterior cuts (blue) were performed to evaluate forces acting in both directions. (H-L) Anaphase. (H,I) Position of the anaphase spindle in wild-type (H) and *chc-1*(*RNAi*) (I) embryos. Spindle poles are marked with red (anterior) and blue (posterior) asterisks. See also supplementary material Movies 1 and 2. (J,K) Anterior (red) and posterior (blue) spindle pole positions during anaphase in embryos shown in H and I. Spindle poles were tracked for 1 min before cytokinesis onset at a frame rate of 5 s. Dashed gray oval lines represent the embryo, black asterisks mark the initial position of the spindle poles. (L) Average peak velocities of anterior (red) and posterior (blue) spindle poles after spindle severing in wild-type and *chc-1*(*RNAi*) embryos. *n*=10 embryos each from three experiments. (M) Quantification of the position of centrosomes at the end of centration, NEBD or the onset of cytokinesis in wild-type (black lines) and *chc-1*(*RNAi*) embryos (gray lines). The position of the anterior (red) and the posterior (blue) MTOCs was projected onto the AP axis of the embryo. Filled lines indicate the spindle, the dashed line the shortest path between the two centrosomes. *n*=10 embryos each from three experiments.

Development (2014) 141, 2712-2723 doi:10.1242/dev.107508

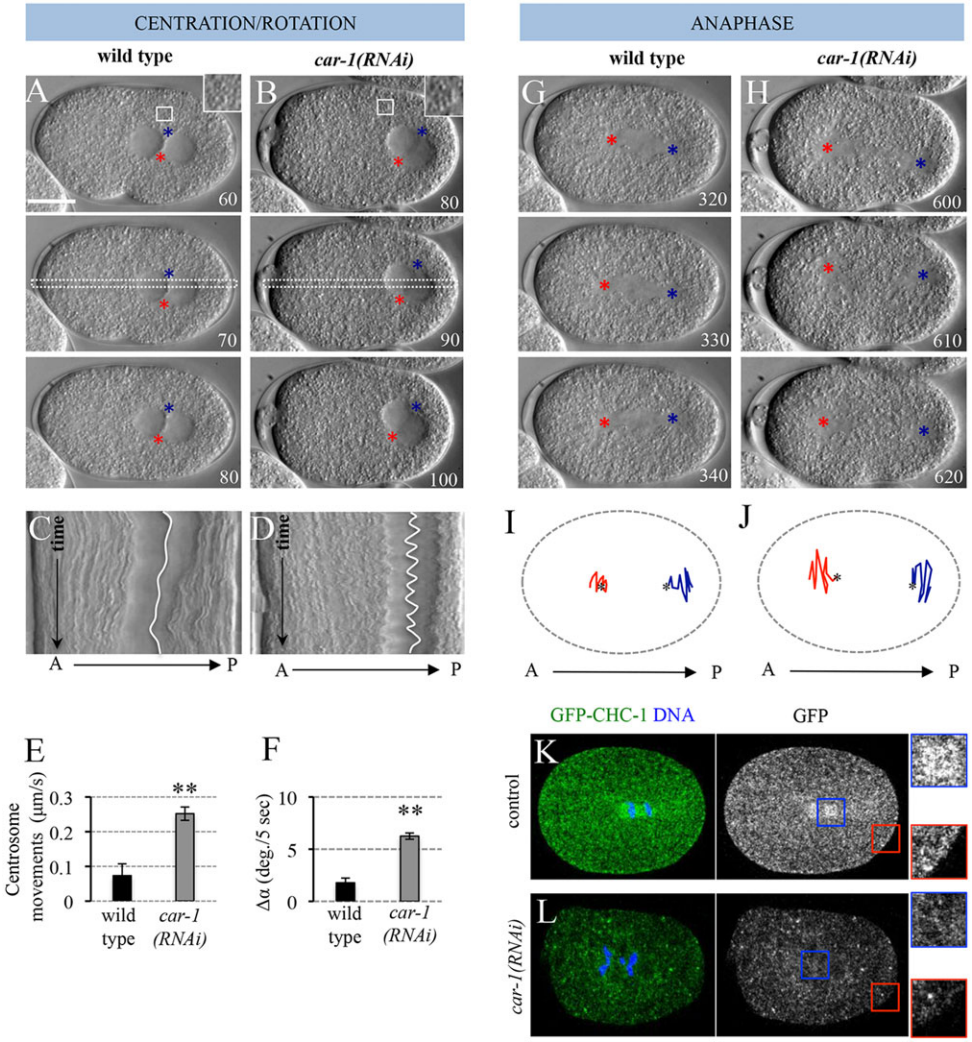

Fig. 2. CAR-1 negatively regulates centrosome/spindle positioning and is needed for normal CHC-1 levels. (A-F) Centration/rotation. (A,B) Centrosome position in wild-type (A) and *car-1*(*RNAi*) (B) embryos monitored by time-lapse DIC microscopy. Centrosomes are marked with red and blue asterisks. Insets show that yolk granules are present normally in *car-1*(*RNAi*) embryos. Note that cell cycle progression is delayed in *car-1*(*RNAi*) embryos. See also supplementary material Movie 3. (C,D) See legend of Fig. 1C,D. Because of the delay in cell cycle progression, only the first 3 min of centration/rotation are shown in *car-1*(*RNAi*) embryos, although excess movements are present throughout centration/rotation (see supplementary material Movie 3). (E,F) Average centrosomal movements (E) and average angular displacement (F) in wild-type and *car-1*(*RNAi*) embryos. See also supplementary material Fig. S1A. *n*=10 embryos from three experiments in every case. (G-J) Anaphase. (G,H) Position of the anaphase spindle in wild-type (G) and *car-1*(*RNAi*) (H) embryos. Centrosomes are marked with red (anterior) and blue (posterior) asterisks. (I,J) Anterior (red) and posterior (blue) spindle pole positions during anaphase in the embryos shown in G and H. Spindle poles were tracked for 1 min before cytokinesis onset at a frame rate of 5 s. Dashed grey oval lines represent the embryo, black asterisks mark the initial position of the spindle poles. (K,L) Immunofluorescence analysis of control (K) and *car-1*(*RNAi*) (L) embryos expressing GFP-CHC-1, stained with antibodies against GFP (green on the left, gray on the right); DNA is seen in blue. Insets display magnified region of the spindle (blue box) and cortex (red box).

GFP-CHC-1 are markedly reduced in *car-1*(*RNAi*) embryos (Fig. 2L; supplementary material Fig. S1L). How CHC-1 levels depend on CAR-1 function remains to be investigated but, regardless of the mechanism, this requirement is not bidirectional, as CAR-1 levels and distribution appear unaffected in *chc-1*(*RNAi*) embryos (supplementary material Fig. S1M,N). Moreover, we observed that yolk granules are not altered in *car-1*(*RNAi*) embryos (Fig. 2B, inset), further demonstrating that the *chc-1*(*RNAi*) MTOC positioning phenotype is not due to depletion of yolk granules.

Overall, we conclude that CAR-1 is needed for appropriate CHC-1 levels in the early embryo. As the above results indicate that the CAR-1 phenotype can be explained by the impact on CHC-1, we investigated the *chc-1*(*RNAi*) phenotype in more detail to uncover how clathrin negatively regulates pulling forces.

Higher forces in *chc-1*(*RNAi*) do not arise from increased levels of cortical force generators

We set out to determine the root of the higher net pulling force phenotype upon CHC-1 depletion. We tested whether polarity is affected, but found that the distribution of P-granules is not changed in *chc-1*(*RNAi*) embryos (supplementary material Fig. S1D,E). Given the role of clathrin in organizing spindle pole structure in human cells (Foraker et al., 2012), we also investigated whether MTOC structure is altered in *chc-1*(*RNAi*) embryos. However, staining with antibodies against the MTOC component TAC-1 (Bellanger and Gönczy, 2003; Le Bot et al., 2003; Srayko et al., 2003) did not reveal a difference compared with wild-type during either centration/rotation or mitosis (supplementary material Fig. S1H-K).

Development (2014) 141, 2712-2723 doi:10.1242/dev.107508

The *chc-1*(*RNAi*) phenotype bears similarity with that of embryos depleted of Gβγ, in which cortical levels of ternary complex components and of dynein are increased because more Gα is available for interaction with GPR-1/2 (Tsou et al., 2003; Afshar et al., 2004). Therefore, we set out to test whether decreased cortical GPB-1 may be what causes the MTOC phenotype in *chc-1*(*RNAi*) embryos. We did find that cortical GPB-1 is diminished in *chc-1*(*RNAi*) embryos both during centration/rotation and mitosis (supplementary material Fig. S2A,B,G,H). Instead, GPB-1 accumulates in intracellular punctae that are RAB-7 positive (supplementary material Fig. S2N), indicating that clathrin is required for GPB-1 trafficking. However, unexpectedly considering the observed diminution of cortical GPB-1, we found that cortical levels of LIN-5 and of the dynein heavy chain DHC-1 are not increased in *chc-1*(*RNAi*) embryos (supplementary material Fig. S2C-F,I-M). This observation suggests that clathrin also promotes the presence of the ternary complex and of dynein at the cell cortex. Overall, the above analysis failed to explain why there is an increase in net pulling forces upon CHC-1 depletion.

Given that depletion of CHC-1 gives rise to a particularly striking phenotype during centration/rotation, we focused further analysis on this stage and asked whether the excess back and forth movements observed in *chc-1*(*RNAi*) embryos requires the function of cortical force generators. To this end, we depleted simultaneously CHC-1 and individual components of the ternary complex. As shown in supplementary material Fig. S3A-J, we found that impairing the function of GOA-1, GPA-16, GPR-1/2 or LIN-5 suppresses excess centrosome movements during centration/rotation in *chc-1*(*RNAi*) embryos. We conclude that although cortical levels of force generator components are not augmented in *chc-1*(*RNAi*) embryos, the increase in net pulling forces is somehow dependent on cortical force generators.

Clathrin is needed for proper organization and tension of the cortical acto-myosin network

As clathrin is known to organize the actin network in other systems (Calabia-Linares et al., 2011; Humphries et al., 2012), we explored whether CHC-1 depletion affects the acto-myosin network in early *C. elegans* embryos. To this end, we performed spinning disk microscopy imaging of the cortical acto-myosin network in live embryos expressing GFP::MOE to visualize filamentous (F) actin. As reported previously (Velarde et al., 2007) and shown in Fig. 3A, we observed small F-actin foci at the time of pronuclear meeting in the anterior of control embryos. Strikingly, we found that CHC-1 depletion results in larger cortical F-actin foci (Fig. 3B,C). We similarly imaged embryos expressing GFP-NMY-2 to visualize non-muscle myosin. We found that instead of the large foci normally present in the anterior of control embryos (Fig. 3D,F) (Munro et al., 2004), *chc-1*(*RNAi*) embryos harbor smaller foci (Fig. 3E,F). Overall, we conclude that the acto-myosin network, whilst not absent, is perturbed upon CHC-1 depletion.

Next, we tested whether such altered organization of the cortical acto-myosin network is accompanied by diminished cortical tension. To this end, we performed cortical laser ablation (COLA) experiments at pronuclear formation (Mayer et al., 2010). In this assay, cortical tension is deduced from measuring the outward velocities of GFP-NMY-2 foci following a laser cut along the longitudinal axis of the embryo (Fig. 4A). As can be seen in supplementary material Fig. S4A-C and Movies 4 and 5, these experiments demonstrated that *chc-1*(*RNAi*) embryos exhibit significantly lower outward velocities compared with the control at pronuclear formation. We next tested whether such a decrease persists into prophase when the most dramatic phenotypic manifestations take place in *chc-1*(*RNAi*) embryos. Because cortical levels of NMY-2-GFP are low at this stage, we performed COLA experiments using embryos expressing GFP::MOE, which give rise to a stronger fluorescence signal at this time. Importantly, these experiments established that there is a likewise significant decrease in cortical tension during centration/rotation compared with the control (Fig. 4B-D; supplementary material Movies 6 and 7). These experiments taken together indicate that clathrin is needed for proper organization and cortical tension of the acto-myosin network in one-cell *C. elegans* embryos.

Alterations in the acto-myosin network probably cause the centrosome positioning phenotype of *chc-1*(*RNAi*) embryos

We reasoned that if the increase in net pulling forces upon CHC-1 depletion is a consequence of defective acto-myosin organization,

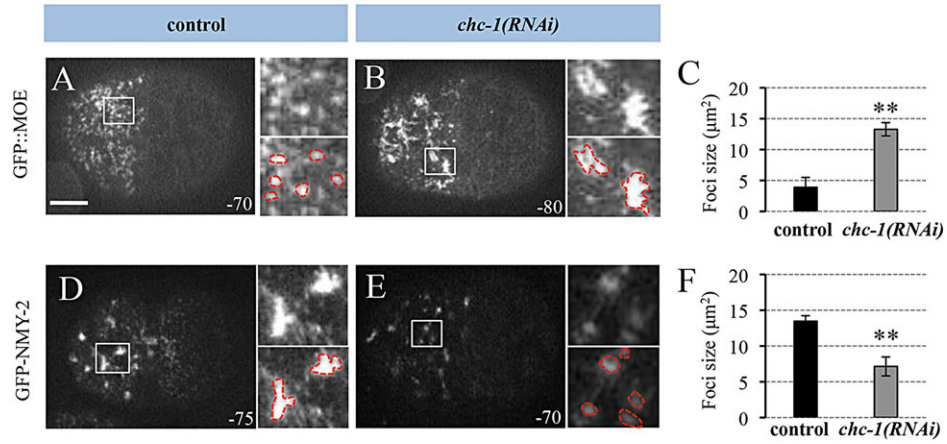

Fig. 3. Clathrin is needed for proper organization of the acto-myosin network in early *C. elegans* embryos. (A,B) Cortical imaging of control (A) and *chc-1*(*RNAi*) (B) embryos expressing the actin-binding fusion protein GFP::MOE visualized with spinning disk microscopy at the onset of pronuclear migration. Insets show magnified cortical regions; some actin foci are delineated in red. (C) Quantification of GFP::MOE foci size in control and *chc-1*(*RNAi*) embryos; *n*=8 embryos each from three experiments, eight to ten foci per embryo. (D,E) Cortical imaging of control (D) and *chc-1*(*RNAi*) (E) embryos expressing GFP-NMY-2 imaged as above. Insets show magnified region of the cortex; GFP-NMY-2 foci are delineated in red. Note that GFP-NMY-2 intensities are lower in *chc-1*(*RNAi*) embryos. (F) Quantification of GFP-NMY-2 foci size in control and *chc-1*(*RNAi*) embryos. Apart from the difference in size, there is an apparent drop in intensity of the foci in *chc-1*(*RNAi*); *n*=8 embryos each from three experiments, eight to ten foci per embryo.

Development (2014) 141, 2712-2723 doi:10.1242/dev.107508

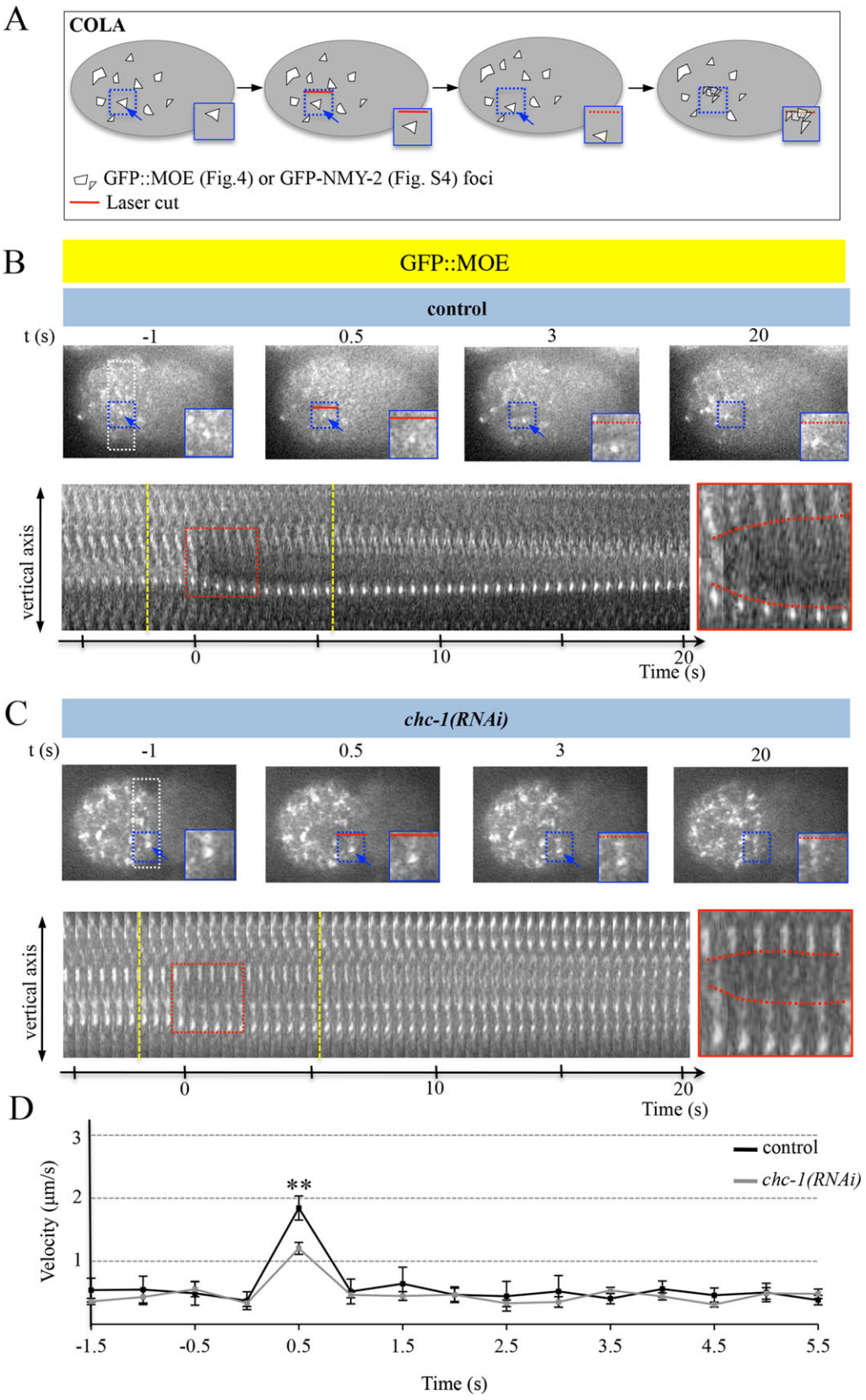

Fig. 4. Clathrin contributes to cortical tension in *C. elegans* embryos. (A) Principle of COLA. Following a longitudinal laser cut in the acto-myosin cell cortex (red line), the movement of GFP::MOE or GFP-NMY-2 foci (white structures) is monitored. Blue arrows point to one specific focus, whose motion (blue dashed rectangle) is magnified in the insets; the red line marks the position of the cut. The resulting outward velocity is an indirect measure of cortical tension (Mayer et al., 2010). (B,C) COLA in control (B) and *chc-1* (*RNAi*) (C) embryos expressing GFP::MOE. Four images from a movie monitoring the cell cortex using spinning disk microscopy are shown, with *t*=0 corresponding to the time of cut. Blue arrows mark a specific GFP::MOE focus; the red line indicates the cut. The cortex is monitored until the complete recovery of GFP::MOE; the inset in the last frame shows the sealed cortex with the tracked focus coalesced. Below are the kymographs constructed from the area marked by the white rectangle, with the area contoured with the red dashed box magnified on the right to better appreciate the outwards motion (dashed red lines within the box indicate the front of the outward movement). (D) Quantification of initial outward velocities from 1.5 s before to 5.5 s after the cut (indicated with dashed yellow lines on the kymographs); *n*=9 embryos each from three experiments were analyzed, see supplementary material Table S2 for statistical analysis. See also corresponding supplementary material Movies 6 and 7.

then stabilizing the actin cytoskeleton should rescue the centrosome positioning phenotype of *chc-1*(*RNAi*) embryos. Jasplakinolide is a macrocyclic peptide that promotes F-actin formation by stimulating filament nucleation (Bubb et al., 1994). We subjected embryos to Jasplakinolide during centration/rotation by piercing holes on the eggshell using the laser microbeam, thus ensuring temporal control to drug exposure and avoiding potential complications due to earlier requirements of the acto-myosin network in AP polarity. Strikingly, we found that whereas the drug does not alter centrosome movements in the wild type (Fig. 5, compare A with E and B

Development (2014) 141, 2712-2723 doi:10.1242/dev.107508

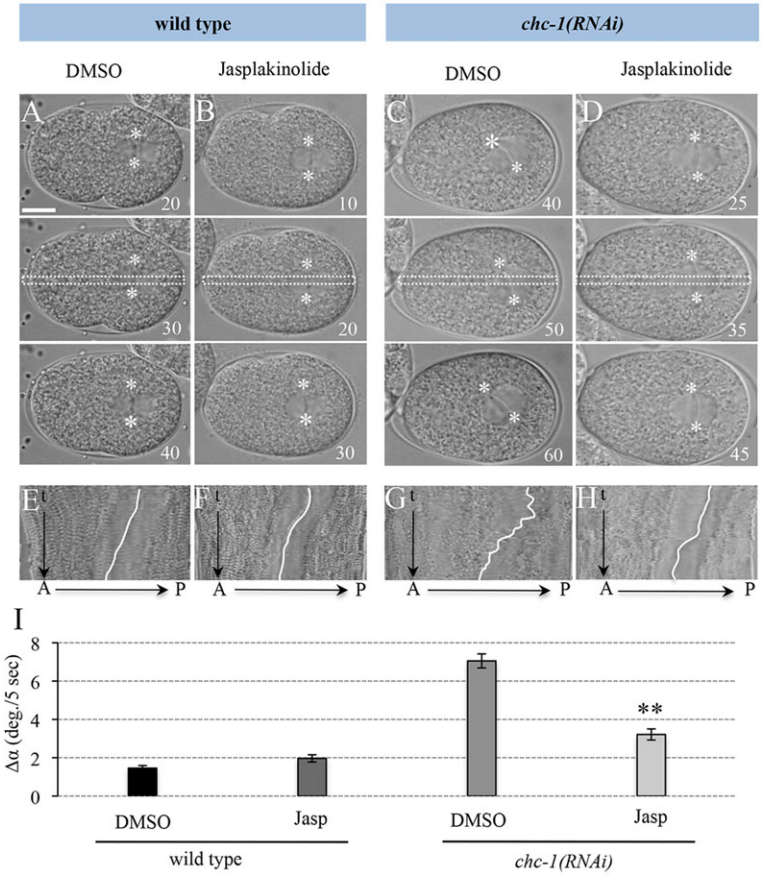

Fig. 5. Stabilizing the acto-myosin network alleviates the *chc-1*(*RNAi*) centration/rotation phenotype. (A-D) Centration/rotation in control (A,B) and *chc-1*(*RNAi*) (C,D) embryos treated with 0.5% DMSO (A,C) or 70 μM Jasplakinolide in 0.5% DMSO (B,D) and monitored by time-lapse microscopy. Centrosomes are marked with white asterisks. Note that the image quality is less good on this microscope equipped with the laser microbeam needed to pierce the eggshell; the same holds for Fig. 6A-C. (E-H) Kymographs corresponding to the white rectangle depicted in A-D. (I) Angular displacement of centrosomes in all experimental conditions; *n*=10 embryos each from three experiments in each case. Note that treating *chc-1*(*RNAi*) embryos with DMSO alone leads to a slight drop in the angular displacement compared to untreated *chc-1*(*RNAi*) embryos (see Fig. 1F). Statistical analysis was performed comparing DMSO and Jasplakinolide treatments, see supplementary material Table S2 for the exact values. Note also that Jasplakinolide led to defective cytokinesis of *chc-1*(*RNAi*), but not control, embryos (data not shown), suggesting that CHC-1 depletion sensitizes embryos to acto-myosin perturbations.

with F), Jasplakinolide alleviates excess movements of *chc-1*(*RNAi*) embryos (Fig. 5C-I). We observed an analogous rescue during anaphase (data not shown). We conclude that alterations in the acto-myosin network are likely to be responsible for the MTOC positioning phenotype of embryos depleted of clathrin.

The above findings raise the possibility that small alterations in the acto-myosin network in otherwise wild-type embryos might result in centrosome positioning phenotypes reminiscent of those observed in *chc-1*(*RNAi*) embryos. We tested this prediction in two ways. First, we subjected embryos to increasing concentrations of the F-actin destabilizing drug Latrunculin A (LatA) during centration/rotation. Whereas treating embryos with high concentration of LatA (240 μM) completely depolymerizes actin as judged by GFP::MOE cortical imaging (compare supplementary material Fig. S4D,F), lower levels of the drug (20 μM) lead to an accumulation of GFP::MOE foci analogous to that observed in *chc-1*(*RNAi*) embryos (supplementary material Fig. S4E,G). Moreover, we found that embryos exposed to low (10 μM) or high (240 μM) concentrations of LatA are indistinguishable from control embryos with respect to centrosome positioning (Fig. 6A,D and 6C,F, quantified in 6G). In sharp contrast, embryos subjected to intermediate concentrations (20 μM and 50 μM) of the drug exhibit excess back and forth movements of centrosomes and excess angular displacement (Fig. 6B,E, quantified in 6G).

As a second means to impart small alterations to the acto-myosin network, we utilized embryos homozygous for the fast inactivating temperature-sensitive allele *nmy-2*(*ne3409*), which is indistinguishable from the wild type at the permissive temperature of 16°C and from *nmy-2*(*RNAi*) at the restrictive temperature of 25°C (Liu et al., 2010). We reasoned that we might observe a centrosome positioning phenotype at intermediate temperatures. As shown in Fig. 6H-M, we indeed found excess centrosome movements during centration/rotation at 20°C, with a corresponding increased angular displacement (Fig. 6N). Overall, we conclude that slight impairment of the acto-myosin network leads to a centrosome positioning phenotype analogous to that observed after depleting clathrin.

2D computational model of centrosome movements during prophase

How can partial impairment of the acto-myosin network result in higher net pulling forces on MTOCs in a manner that depends on cortical force generators? It has been proposed that, during anaphase, depolymerizing microtubules bound to cortical force generators exert a pulling force proportional to the rigidity of the cell cortex, which is related to its tension (Kozlowski et al., 2007). We considered an analogous mechanism during prophase, which is illustrated in Fig. 7A and summarized hereafter. When a microtubule bound to a cortical force generator depolymerizes, the cortex is stretched and responds with a force that is proportional to its rigidity and to the stretch. Moreover, the rate at which the motor eventually detaches from the cortex depends exponentially on the applied force. With high cortical rigidity, the total force is high and detachment occurs relatively fast. With medium cortical rigidity, a less intense force is generated at once but for a longer time before detachment occurs, resulting in higher total work. When cortical rigidity is weak, the limit in the maximum stretching of the cortex or the membrane is reached and detachment occurs without much force generation.

We developed a minimal 2D computational model of stochastic prophase centrosome movements driven by cortical force generators that encapsulates the essence of the above mechanism (Fig. 7B-F;

Development (2014) 141, 2712-2723 doi:10.1242/dev.107508

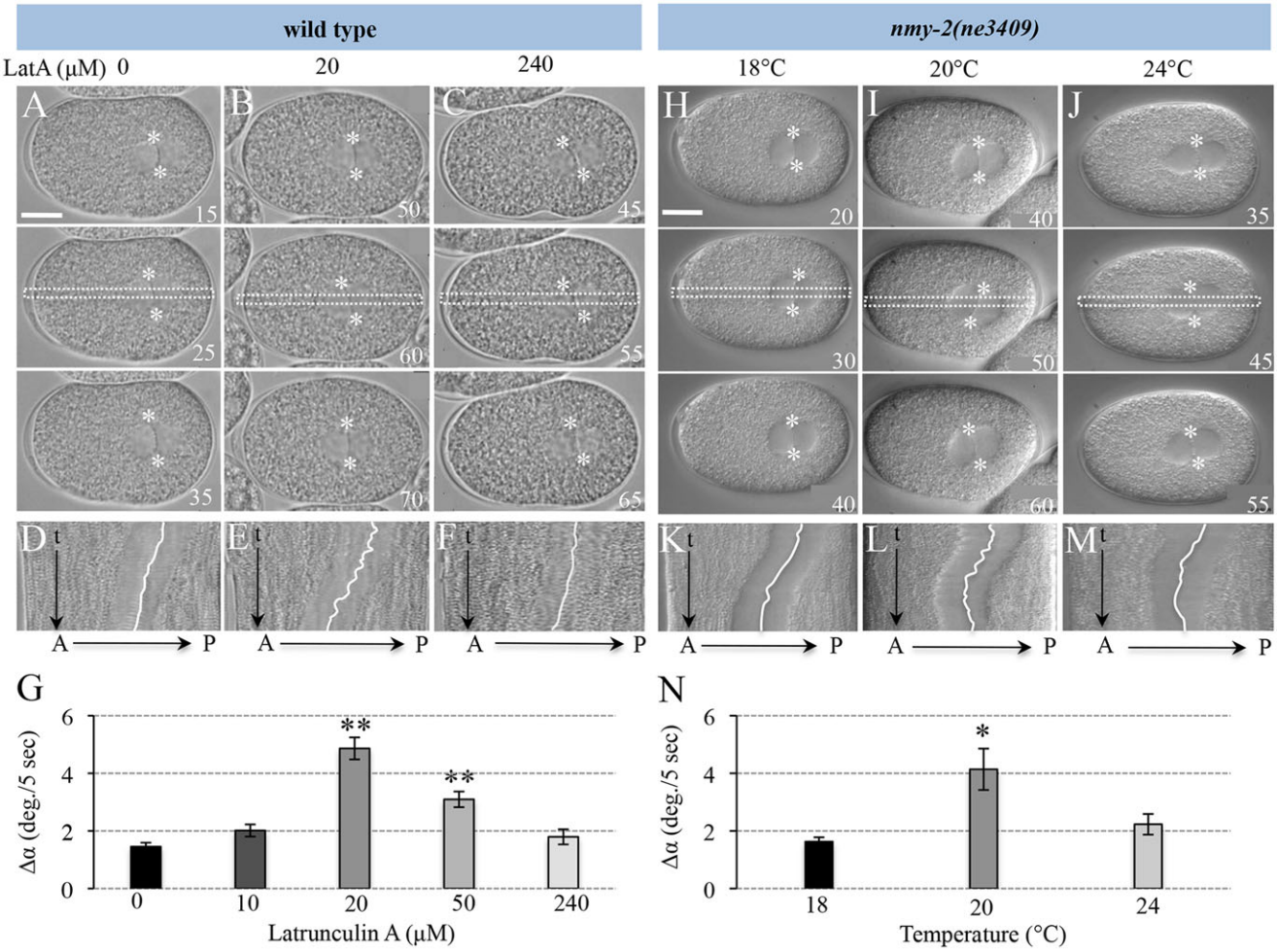

Fig. 6. Partial disruption of the acto-myosin network resembles the *chc-1(RNAi)* phenotype. (A-C) Centration/rotation in embryos treated with 0 (A), 20 (B) or 240 (C) μM Latrunculin A and monitored by time-lapse microscopy. Centrosomes are marked with white asterisks. (D-F) Kymographs corresponding to the white rectangle depicted in A-C. (G) Angular displacement of centrosomes in all experimental conditions; *n*=10 embryos each from three experiments were analyzed. The corresponding DMSO controls did not affect angular displacement (data not shown). (H-J) Centration/rotation in *nmy-2*(*ne3409*) temperature-sensitive embryos imaged with time-lapse DIC microscopy at 18°C (H), 20°C (I) or 24°C (J). (K-M) Kymographs corresponding to the white rectangle depicted in H-J. (N) Angular displacement of centrosomes in all experimental conditions; *n*=10 embryos each from three experiments were analyzed. Note that embryos imaged at 20 and 21°C, as well as 24 and 25°C, were pooled for the analysis. Wild-type embryos at 25°C do not differ from ones at lower temperature in terms of angular displacement (data not shown). See supplementary material Table S2 for statistical analysis and exact values shown in panels G and N.

see methods in the supplementary material). In this model, a rotating disk representing the two pronuclei is fixed in the center of an ellipsoidal embryo and two microtubule asters emanate from two centrosomes at opposite poles of the disk. The microtubules are dynamic, undergoing growth and shrinkage, and can bind to a force generator when abutting the cortex. A pulling force is generated when the microtubule depolymerizes. Parameters for the simulation were set to measured values whenever possible or varied across a reasonable range (supplementary material Table S1). Strikingly, simulations demonstrate that this model predicts maximum oscillation amplitudes for medium values of cortical rigidity (Fig. 7B-E; see also supplementary material Movies 6-8), as evidenced also by plotting the standard deviation of rotational velocity as a function of cortical rigidity (Fig. 7F). Therefore, the model predicts that excess centrosome movements should occur at medium cortical rigidity values, mirroring the phenotypic observations in embryos depleted of CHC-1.

DISCUSSION

In this study, we uncovered the fact that clathrin negatively regulates pulling forces acting on centrosomes and spindle poles in one-cell *C. elegans* embryos. Furthermore, we demonstrated that clathrin maintains proper tension of the acto-myosin cortex, which probably explains how clathrin participates in the control of centrosome positioning.

There are other conditions besides *chc-1*(*RNAi*) in which centrosomes undergo excess back and forth movements during centration/rotation, as well as excess spindle oscillations during anaphase, including upon depletion of GPB-1 or CSNK-1 (Tsou et al., 2003; Afshar et al., 2004; Panbianco et al., 2008). In both cases, the increase in net pulling forces is accompanied by elevated levels of cortical force generators. By contrast, we found that this is not the case in *chc-1*(*RNAi*) embryos and thus inferred that clathrin must modulate force generation by another means. We discovered that this involves the acto-myosin network. We found that the organization and tension of the actin-myosin cortex are impaired upon clathrin depletion in *C. elegans* embryos. This appears to be causative of the *chc-1*(*RNAi*) MTOC positioning phenotype, as stabilizing the actin cytoskeleton alleviates these phenotypic manifestations. The contribution of clathrin for an intact acto-myosin network has been reported in other systems. Thus, clathrin

Development (2014) 141, 2712-2723 doi:10.1242/dev.107508

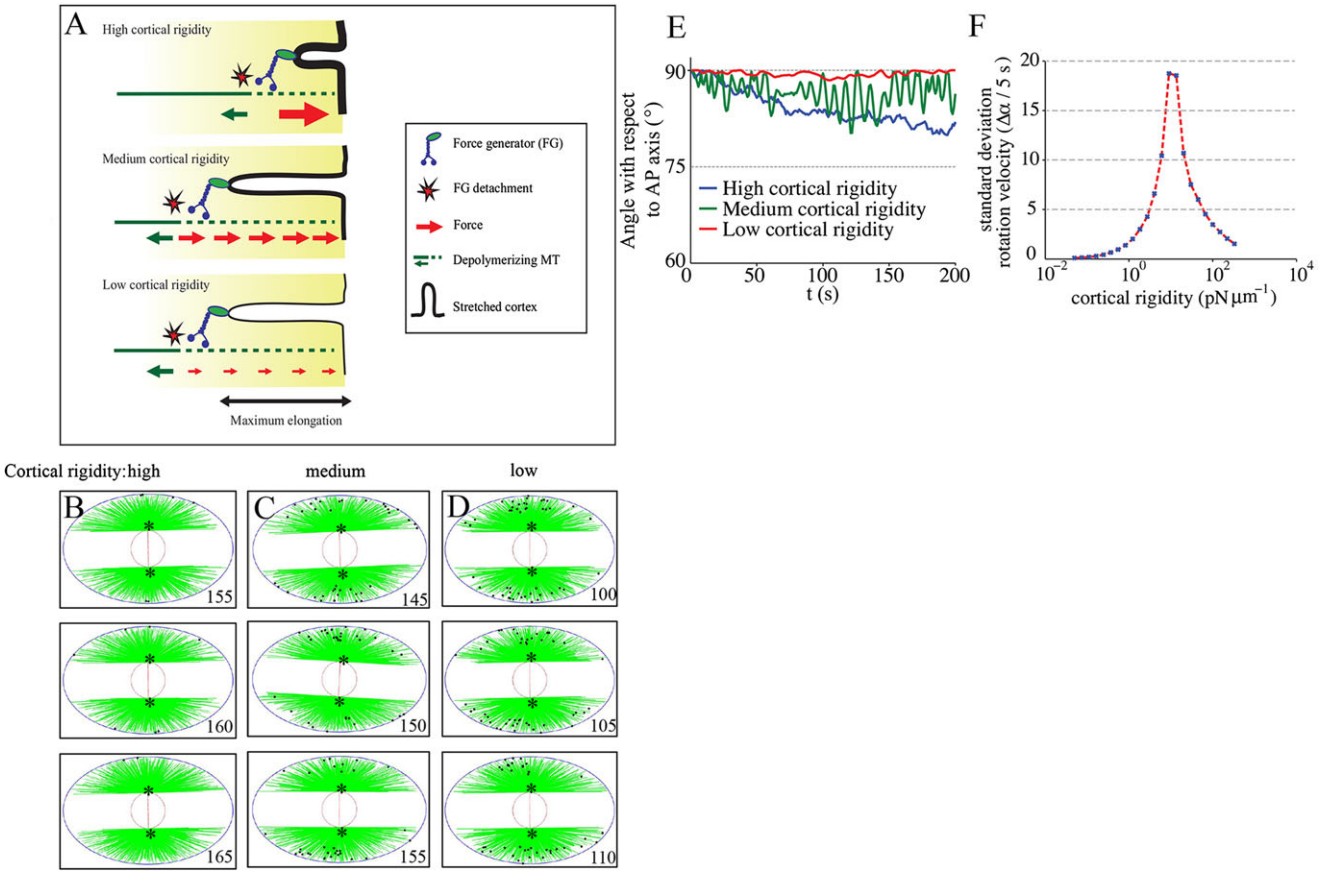

Fig. 7. 2D computational model of centrosome oscillations. (A) Model of cortical force generation. The depolymerizing microtubule bound to a cortical force generator stretches the cortex and thus experiences a pulling reaction force. For high cortical rigidity, a strong elastic force is applied, but the force generator detaches rapidly. For medium cortical rigidity, the stretch reaches the maximum elongation before the force generator detaches, resulting in high total forces (i.e. work). For low cortical rigidity, the stretch also reaches the maximum elongation, but the cortex is too loose to apply a large force. (B-D) Simulation of stochastic centrosome movements driven by cortical force generators. Representative frames of simulated movements are shown for high, medium and low cortical rigidity (frame rate 5 s). (E) Representative simulations of stochastic centrosome movements with high (blue), medium (green) or low (red) cortical rigidity (100, 10 and 1 pN μm^{-1}, respectively). The centrosome axis is perpendicular to the AP axis. (F) Standard deviation of the angular velocity of the simulated pronuclear oscillations as a function of cortical rigidity. The angular velocity is calculated over time steps of 5 s. *n*=30 simulations for each cortical rigidity value. See also supplementary material Movies 8–10.

located on endosomes plays a role in organizing the actin network at the immunological synapse in T-cells (Calabia-Linares et al., 2011). Moreover, clathrin is needed for actin polymerization promoted by vaccinia viral infection (Humphries et al., 2012). Our findings contribute to this body of work and underscore the influence of clathrin on acto-myosin function in a range of biological settings. The interaction between clathrin and actin in other systems occurs via the clathrin light chain and the huntingtin interacting protein 1 related (*hipr-1* in *C. elegans*) (Poupon et al., 2008; Wilbur et al., 2008; Boettner et al., 2011). However, we found that neither the depletion of the clathrin light chain *clic-1* nor of *hipr-1* leads to MTOC positioning defects (data not shown). This raises the possibility that there may be a novel mechanism through which the clathrin heavy chain interacts with actin in *C. elegans*.

Is clathrin-dependent modulation of the acto-myosin network distinct from its well-known role in endocytosis? A definite answer to this important question is difficult to obtain. First, endocytosis in general affects the actin cytoskeleton and reciprocally, making it challenging to analyze the two processes separately (reviewed by Galletta and Cooper, 2009). Second, inhibiting endocytosis in one-cell *C. elegans* embryos using a dynamin mutant results in lower levels of cortical GPB-1, thus probably influencing force generation via increased cortical dynein (Thyagarajan et al., 2011). This could explain the clathrin-like centration/rotation phenotype observed upon depletion of the early endosomal protein RAB-5 (Hyenne et al., 2012). Note also that RAB-5 localization is slightly affected in *chc-1*(*RNAi*) embryos (Audhya et al., 2007), but whether CHC-1 may be altered upon RAB-5 depletion is not known. Despite these limitations, our results lead us to favor the view that the impact of clathrin on MTOC is uncoupled from its role in endocytosis. Indeed, we found that *rme-2*(*RNAi*) embryos, in which endocytosis is altered, does not exhibit an MTOC positioning phenotype. Conversely, *car-1*(*RNAi*) embryos, in which endocytosis is not altered, but in which CHC-1 levels are compromised, exhibit an MTOC positioning phenotype analogous to that of *chc-1*(*RNAi*) embryos.

An involvement of the acto-myosin network during centration/rotation has been proposed previously (Goulding et al., 2007). Based on the movements of cortical foci of NMY-2-GFP, it was hypothesized that acto-myosin-derived forces can be directed towards either the anterior or the posterior of the embryo, and that LET-99 favors anterior-directed movements and thus centration (Goulding et al., 2007). Although there might be a slight mislocalization of LET-99 in *chc-1*(*RNAi*) embryos, perhaps as a result of perturbations in the acto-myosin cytoskeleton (data not

Development (2014) 141, 2712-2723 doi:10.1242/dev.107508

shown), the centration/rotation phenotype of *chc-1*(*RNAi*) embryos is not suppressed by removing LET-99 (data not shown), indicating that LET-99 mislocalization cannot be causative in this case.

How, then, can perturbations in the acto-myosin network lead to the generation of higher net pulling forces acting on centrosomes and spindle poles of one-cell *C. elegans* embryos? We found that the angular displacement of centrosomes during centration/rotation differs from the wild type only when the acto-myosin network is disturbed slightly, but not when it is compromised more severely. These observations are consistent with predictions from 3D simulations of anaphase spindle positioning, whereby medium levels of cortical rigidity were predicted to result in increased oscillations compared with either lower or higher cortical rigidity (Kozlowski et al., 2007). Inspired by this work, we set out to model centrosome movements during prophase as a function of cortical rigidity. We were able to simulate the experimental data, whereby medium cortical rigidity results in maximal centrosome oscillations. The rationale behind this force curve is that a cortex with medium rigidity, as in *chc-1*(*RNAi*) embryos, can stretch more upon being pulled while maintaining the interaction between the force generator and the depolymerizing microtubule, leading to higher total work (Fig. 7A). We note that large membrane invaginations are indeed observed in embryos that are likely to have impaired cortical rigidity as a result of partial depletion of NMY-2, although overall spindle positioning appears to be unaffected in such embryos, as in *chc-1* (*RNAi*) embryos (Redemann et al., 2010).

Does the model we propose here for centration/rotation apply during anaphase? Intriguingly, treating mitotic embryos with the actin-depolymerizing agent Latrunculin A leads to an increase of net forces pulling on the anterior spindle pole (Afshar et al., 2010; Berends et al., 2013). However, this is the case either with high (Afshar et al., 2010; Berends et al., 2013) or intermediate (data not shown) levels of Latrunculin A. Although it may be that the effective drug concentration inside the embryo is lower during mitosis, thus resulting in medium cortical rigidity even with high levels of the drug, future work will be needed to elucidate whether the mechanisms at play during centration/rotation apply during anaphase.

A requirement for balanced levels of cortical tension may extend to human cells, in which perturbation of the acto-myosin network also affects spindle positioning on a uniform fibronectin substrate (Toyoshima and Nishida, 2007). It would be interesting to test whether the depletion of clathrin likewise affects spindle positioning in that system. We note that the cortical acto-myosin network also plays a crucial role during asymmetric division of Q neuroblast in *C. elegans*, where asymmetric contractile forces are key for generating daughter cells of different sizes (Ou et al., 2010). Our findings further indicate that modulation of cortical tension can be harnessed to ensure proper centrosome positioning in different biological systems.

MATERIALS AND METHODS

Worm strains and RNAi

Transgenic worms expressing GFP-RAB-7 (a gift from Barth Grant, Rutgers University, Piscataway, USA), GFP-NMY-2 (Munro et al., 2004), GFP::MOE (Velarde et al., 2007) or GFP-CHC-1 (Greener et al., 2001) were maintained at 24°C. The *nmy-2*(*ne3409*) temperature-sensitive strain (Liu et al., 2010) was kept at 16°C, dissected in M9 stored at the same temperature and shifted to the indicated temperatures at the time of pronuclear meeting.

RNAi bacterial feeding strains for *gpr-1/2* and *gpa-16* were described (Colombo et al., 2003), as were those for *rme-2* and *car-1* (Rual et al., 2004). RNAi was performed by feeding L3-L4 animals at 24°C for 20-24 h for *chc-1*, *car-1* and *rme-2*, or at 20°C for 48 h for *gpr-1/2* and *gpa-16*.

Antibodies, western blotting and indirect immunofluorescence

Sodium dodecyl sulfate-polyacrylamide gel electrophoresis (SDS-PAGE) and western blot analyses were performed according to standard protocols. Antibodies against GFP (Roche, mouse, 1/500; 11814460001), CAR-1 [a gift from Karen Oegama (Ludwig Insitute for Cancer Research, San Diego, USA) and Jon Audhya (University of Wisconsin, Madison, USA) (Audhya et al., 2005) rabbit, 1/1000] and α-tubulin (DM1A, Sigma, mouse, 1/2000) were used as primary antibodies. HRP-conjugated goat anti-rabbit and anti-mouse secondary antibodies (Promega) were used at 1/5000 and the signal detected using standard chemiluminescence (Roche).

For immunostaining, embryos were fixed in methanol at −20°C for 1 h, followed by overnight incubation at 4°C with primary antibodies. Primary mouse antibodies against α-tubulin (1/300; DM1A, Sigma), GFP (1/100; MAB3580, Millipore) were used together with rabbit antibodies against GPB-1 (1/200; Thyagarajan et al., 2011), LIN-5 (1/300; Nguyen-Ngoc et al., 2007), DHC-1 (1/100; Kotak et al., 2012), PGL-1 (1/300; Kawasaki et al., 1998) or TAC-1 (1/500; Bellanger and Gönczy, 2003). Secondary antibodies were Alexa488-conjugated goat anti-mouse (1:500; Life Technologies, A11001) and Cy3-conjugated goat anti-rabbit (1/1000; Jackson ImmunoResearch, 711-165-152). Slides were counterstained with 1 mg/ml Hoechst 33258 (Sigma) to visualize DNA. Images were acquired on an LSM700 confocal microscope (Zeiss) and processed in ImageJ and Adobe Photoshop, maintaining relative image intensities within a series.

Microscopy, spindle severing, drug treatment and image analysis

Embryos were observed by time-lapse DIC microscopy as described (Gönczy et al., 1999). Centrosomal movements during centration were determined by automatically tracking the position of the associated pronuclei using a MatLab script computing the average absolute movement of centrosomes every 5 s for ten frames following pronuclear meeting. The average angular displacement during centration/rotation was calculated using ImageJ, with the *x* and *y* coordinates of the two centrosomes computed every 5 s for ten frames after pronuclear meeting. The temperature control device used for imaging *nmy-2*(*ne3409*) embryos was described previously (Nguyen-Ngoc et al., 2007).

Spindle severing experiments were performed essentially as described (Afshar et al., 2004) using a Leica LMD microscope equipped with a pulsed N_2 laser (λ=337 nm). Astral microtubules were severed during centration/rotation either anterior or posterior from the centrosome/pronuclear complex, whereas the spindle was severed at the onset of anaphase. Tracking of the MTOCs and calculation of peak velocities were performed as described (Grill et al., 2001).

For drug treatment, the Leica LMD microscope was used to pierce a hole in the eggshell of pseudocleavage stage embryos bathed in Jasplakinolide (Life Technologies) or Latrunculin A (Merck Millipore), both resuspended in 0.5% DMSO. Embryos were then imaged every 5 s until the end of the first cell cycle.

Imaging of NMY-2-GFP and GFP::MOE was performed using an inverted Zeiss Axiovert 200 microscope with a 60×1.4 NA lens, acquiring cortical images with a COOLSNAP HQ B/W camera every 500 ms using 250 ms excitation with a 488 nm solid state laser. Transmission light was used every minute to unambiguously identify the embryo stage. We used ImageJ to manually mark cortical foci and determine their size, applying an empirical threshold to distinguish between two foci; eight to ten foci were analyzed per embryo.

For COLA experiments (Mayer et al., 2010), we used an inverted Zeiss Axiovert 200 microscope equipped with a 355 nm pulsed UV laser for ablation. Images were acquired with a frame rate of 500 ms using 250 ms excitation time with a 488 nm argon laser. The ∼10 µm ablation was performed on the anterior cortex along the longitudinal axis either at pronuclear formation (GFP-NMY-2 embryos) or at the onset of centration/rotation (GFP::MOE embryos). Only those embryos in which the cut sealed and that divided normally were analyzed. We used ImageJ to manually track the foci over 15 frames (three prior to the cut and 11 afterwards) and

calculate their velocity (tracking five to ten foci or two or three foci per embryo for GFP-NMY-2 and GFP::MOE, respectively). The mean velocity per embryo was averaged and plotted over time. Statistical analysis was performed on the velocities measured 500 ms after the cut. The values reported here for control embryos during pronuclear migration are larger than in the literature (Mayer et al., 2010), most likely because in the previous work imaging began only 5 s after the cut, compared with 500 ms here.

Simulation

See methods in the supplementary material for modeling details.

Acknowledgements

We thank Barth Grant, Craig Mello, Ed Munro, Karen Oegema and Jon Audhya, as well as Fabio Piano for worm strains and Susan Strome for PGL-1 antibodies. We are grateful to Aitana Neves da Silva for writing the MatLab script for tracking pronuclei, to Stephan Grill for advice with the COLA assay, to François Nédélec for discussions on the modeling, to the EPFL School of Life Sciences microscopy core facility (BiOP) for advice, as well as to Fernando R. Balestra, Daniel Constam, Virginie Hamel Hachet and Sachin Kotak for comments on the manuscript. Some strains were obtained from the *Caenorhabditis* Genetics Center, which is funded by the NIH National Center for Research Resources (NCRR).

Competing interests

The authors declare no competing financial interests.

Author contributions

Z.S., A.D.S., K.T., K.A. and P.G. designed aspects of the project; Z.S., K.T., A.D.S., K.A. and S.T. conducted experiments; all authors analyzed data; Z.S., A.D.S. and P.G. wrote the manuscript.

Funding

Supported by a grant from the Swiss National Science Foundation [3100A0-122500/1].

Supplementary material

Supplementary material available online at
http://dev.biologists.org/lookup/suppl/doi:10.1242/dev.107508/-/DC1

References

Afshar, K., Willard, F. S., Colombo, K., Johnston, C. A., McCudden, C. R., Siderovski, D. P. and Gönczy, P. (2004). RIC-8 is required for GPR-1/2-dependent Galpha function during asymmetric division of C. elegans embryos. *Cell* **119**, 219-230.

Afshar, K., Werner, M. E., Tse, Y. C., Glotzer, M. and Gönczy, P. (2010). Regulation of cortical contractility and spindle positioning by the protein phosphatase 6 PPH-6 in one-cell stage C. elegans embryos. *Development* **137**, 237-247.

Audhya, A., Hyndman, F., McLeod, I. X., Maddox, A. S., Yates, J. R., III, Desai, A. and Oegema, K. (2005). A complex containing the Sm protein CAR-1 and the RNA helicase CGH-1 is required for embryonic cytokinesis in Caenorhabditis elegans. *J. Cell Biol.* **171**, 267-279.

Audhya, A., Desai, A. and Oegema, K. (2007). A role for Rab5 in structuring the endoplasmic reticulum. *J. Cell Biol.* **178**, 43-56.

Bellanger, J.-M. and Gönczy, P. (2003). TAC-1 and ZYG-9 form a complex that promotes microtubule assembly in C. elegans embryos. *Curr. Biol.* **13**, 1488-1498.

Berends, C. W. H., Munoz, J., Portegijs, V., Schmidt, R., Grigoriev, I., Boxem, M., Akhmanova, A., Heck, A. J. R. and van den Heuvel, S. (2013). F-actin asymmetry and the endoplasmic reticulum-associated TCC-1 protein contribute to stereotypic spindle movements in the Caenorhabditis elegans embryo. *Mol. Biol. Cell* **24**, 2201-2215.

Boag, P. R., Nakamura, A. and Blackwell, T. K. (2005). A conserved RNA-protein complex component involved in physiological germline apoptosis regulation in C. elegans. *Development* **132**, 4975-4986.

Boettner, D. R., Friesen, H., Andrews, B. and Lemmon, S. K. (2011). Clathrin light chain directs endocytosis by influencing the binding of the yeast Hip1R homologue, Sla2, to F-actin. *Mol. Biol. Cell* **22**, 3699-3714.

Bubb, M. R., Senderowicz, A. M., Sausville, E. A., Duncan, K. L. and Korn, E. D. (1994). Jasplakinolide, a cytotoxic natural product, induces actin polymerization and competitively inhibits the binding of phalloidin to F-actin. *J. Biol. Chem.* **269**, 14869-14871.

Calabia-Linares, C., Robles-Valero, J., de la Fuente, H., Perez-Martinez, M., Martin-Cofreces, N., Alfonso-Perez, M., Gutierrez-Vazquez, C., Mittelbrunn, M., Ibiza, S., Urbano-Olmos, F. R. et al. (2011). Endosomal clathrin drives actin accumulation at the immunological synapse. *J. Cell Sci.* **124**, 820-830.

Colombo, K., Grill, S. W., Kimple, R. J., Willard, F. S., Siderovski, D. P. and Gönczy, P. (2003). Translation of polarity cues into asymmetric spindle positioning in Caenorhabditis elegans embryos. *Science* **300**, 1957-1961.

Couwenbergs, C., Labbe, J.-C., Goulding, M., Marty, T., Bowerman, B. and Gotta, M. (2007). Heterotrimeric G protein signaling functions with dynein to promote spindle positioning in C. elegans. *J. Cell Biol.* **179**, 15-22.

Foraker, A. B., Camus, S. M., Evans, T. M., Majeed, S. R., Chen, C.-Y., Taner, S. B., Correa, I. R., Jr, Doxsey, S. J. and Brodsky, F. M. (2012). Clathrin promotes centrosome integrity in early mitosis through stabilization of centrosomal ch-TOG. *J. Cell Biol.* **198**, 591-605.

Galletta, B. J. and Cooper, J. A. (2009). Actin and endocytosis: mechanisms and phylogeny. *Curr. Opin. Cell Biol.* **21**, 20-27.

Gönczy, P. (2008). Mechanisms of asymmetric cell division: flies and worms pave the way. *Nat. Rev. Mol. Cell Biol.* **9**, 355-366.

Gönczy, P. and Rose, L. S. (2005). Asymmetric cell division and axis formation in the embryo. *WormBook*, 1-20.

Gönczy, P., Schnabel, H., Kaletta, T., Amores, A. D., Hyman, T. and Schnabel, R. (1999). Dissection of cell division processes in the one cell stage Caenorhabditis elegans embryo by mutational analysis. *J. Cell Biol.* **144**, 927-946.

Gönczy, P., Echeverri, C., Oegema, K., Coulson, A., Jones, S. J. M., Copley, R. R., Duperon, J., Oegema, J., Brehm, M., Cassin, E. et al. (2000). Functional genomic analysis of cell division in C. elegans using RNAi of genes on chromosome III. *Nature* **408**, 331-336.

Gotta, M. and Ahringer, J. (2001). Distinct roles for Galpha and Gbetagamma in regulating spindle position and orientation in Caenorhabditis elegans embryos. *Nat. Cell Biol.* **3**, 297-300.

Gotta, M., Dong, Y., Peterson, Y. K., Lanier, S. M. and Ahringer, J. (2003). Asymmetrically distributed C. elegans homologs of AGS3/PINS control spindle position in the early embryo. *Curr. Biol.* **13**, 1029-1037.

Goulding, M. B., Canman, J. C., Senning, E. N., Marcus, A. H. and Bowerman, B. (2007). Control of nuclear centration in the C. elegans zygote by receptor-independent Galpha signaling and myosin II. *J. Cell Biol.* **178**, 1177-1191.

Grant, B. and Hirsh, D. (1999). Receptor-mediated endocytosis in the Caenorhabditis elegans oocyte. *Mol. Biol. Cell* **10**, 4311-4326.

Greener, T., Grant, B., Zhang, Y., Wu, X., Greene, L. E., Hirsh, D. and Eisenberg, E. (2001). Caenorhabditis elegans auxilin: a J-domain protein essential for clathrin-mediated endocytosis in vivo. *Nat. Cell Biol.* **3**, 215-219.

Grill, S. W., Gönczy, P., Stelzer, E. H. K. and Hyman, A. A. (2001). Polarity controls forces governing asymmetric spindle positioning in the Caenorhabditis elegans embryo. *Nature* **409**, 630-633.

Humphries, A. C., Dodding, M. P., Barry, D. J., Collinson, L. M., Durkin, C. H. and Way, M. (2012). Clathrin potentiates vaccinia-induced actin polymerization to facilitate viral spread. *Cell Host Microbe* **12**, 346-359.

Hyenne, V., Tremblay-Boudreault, T., Velmurugan, R., Grant, B. D., Loerke, D. and Labbé, J.-C. (2012). RAB-5 controls the cortical organization and dynamics of PAR proteins to maintain C. elegans early embryonic polarity. *PLoS ONE* **7**, e35286.

Kawasaki, I., Shim, Y.-H., Kirchner, J., Kaminker, J., Wood, W. B. and Strome, S. (1998). PGL-1, a predicted RNA-binding component of germ granules, is essential for fertility in C. elegans. *Cell* **94**, 635-645.

Knoblich, J. A. (2008). Mechanisms of asymmetric stem cell division. *Cell* **132**, 583-597.

Kotak, S. and Gönczy, P. (2013). Mechanisms of spindle positioning: cortical force generators in the limelight. *Curr. Opin. Cell Biol.* **25**, 741-748.

Kotak, S., Busso, C. and Gönczy, P. (2012). Cortical dynein is critical for proper spindle positioning in human cells. *J. Cell Biol.* **199**, 97-110.

Kozlowski, C., Srayko, M. and Nedelec, F. (2007). Cortical microtubule contacts position the spindle in C. elegans embryos. *Cell* **129**, 499-510.

Krueger, L. E., Wu, J.-C., Tsou, M.-F. B. and Rose, L. S. (2010). LET-99 inhibits lateral posterior pulling forces during asymmetric spindle elongation in C. elegans embryos. *J. Cell Biol.* **189**, 481-495.

Laan, L., Pavin, N., Husson, J., Romet-Lemonne, G., van Duijn, M., López, M. P., Vale, R. D., Jülicher, F., Reck-Peterson, S. L. and Dogterom, M. (2012). Cortical dynein controls microtubule dynamics to generate pulling forces that position microtubule asters. *Cell* **148**, 502-514.

Labbe, J. C., McCarthy, E. K. and Goldstein, B. (2004). The forces that position a mitotic spindle asymmetrically are tethered until after the time of spindle assembly. *J. Cell Biol.* **167**, 245-256.

Le Bot, N., Tsai, M.-C., Andrews, R. K. and Ahringer, J. (2003). TAC-1, a regulator of microtubule length in the C. elegans embryo. *Curr. Biol.* **13**, 1499-1505.

Liu, J., Maduzia, L. L., Shirayama, M. and Mello, C. C. (2010). NMY-2 maintains cellular asymmetry and cell boundaries, and promotes a SRC-dependent asymmetric cell division. *Dev. Biol.* **339**, 366-373.

Mayer, M., Depken, M., Bois, J. S., Jülicher, F. and Grill, S. W. (2010). Anisotropies in cortical tension reveal the physical basis of polarizing cortical flows. *Nature* **467**, 617-621.

Munro, E., Nance, J. and Priess, J. R. (2004). Cortical flows powered by asymmetrical contraction transport PAR proteins to establish and maintain anterior-posterior polarity in the early C. elegans embryo. *Dev. Cell* **7**, 413-424.

Development (2014) 141, 2712-2723 doi:10.1242/dev.107508

Nelson, K. K. and Lemmon, S. K. (1993). Suppressors of clathrin deficiency: overexpression of ubiquitin rescues lethal strains of clathrin-deficient Saccharomyces cerevisiae. *Mol. Cell. Biol.* **13**, 521-532.

Nguyen-Ngoc, T., Afshar, K. and Gönczy, P. (2007). Coupling of cortical dynein and G alpha proteins mediates spindle positioning in Caenorhabditis elegans. *Nat. Cell Biol.* **9**, 1294-1302.

Noatynska, A. and Gotta, M. (2012). Cell polarity and asymmetric cell division: the C. elegans early embryo. *Essays Biochem.* **53**, 1-14.

Noble, S. L., Allen, B. L., Goh, L. K., Nordick, K. and Evans, T. C. (2008). Maternal mRNAs are regulated by diverse P body-related mRNP granules during early Caenorhabditis elegans development. *J. Cell Biol.* **182**, 559-572.

Oegema, K. and Hyman, A. A. (2006). Cell division. *WormBook*, 1-40.

Ou, G., Stuurman, N., D'Ambrosio, M. and Vale, R. D. (2010). Polarized myosin produces unequal-size daughters during asymmetric cell division. *Science* **330**, 677-680.

Panbianco, C., Weinkove, D., Zanin, E., Jones, D., Divecha, N., Gotta, M. and Ahringer, J. (2008). A casein kinase 1 and PAR proteins regulate asymmetry of a PIP(2) synthesis enzyme for asymmetric spindle positioning. *Dev. Cell* **15**, 198-208.

Park, D. H. and Rose, L. S. (2008). Dynamic localization of LIN-5 and GPR-1/2 to cortical force generation domains during spindle positioning. *Dev. Biol.* **315**, 42-54.

Poupon, V., Girard, M., Legendre-Guillemin, V., Thomas, S., Bourbonniere, L., Philie, J., Bright, N. A. and McPherson, P. S. (2008). Clathrin light chains function in mannose phosphate receptor trafficking via regulation of actin assembly. *Proc. Natl. Acad. Sci. U.S.A.* **105**, 168-173.

Rai, A. K., Rai, A., Ramaiya, A. J., Jha, R. and Mallik, R. (2013). Molecular adaptations allow dynein to generate large collective forces inside cells. *Cell* **152**, 172-182.

Redemann, S., Pecreaux, J., Goehring, N. W., Khairy, K., Stelzer, E. H. K., Hyman, A. A. and Howard, J. (2010). Membrane invaginations reveal cortical sites that pull on mitotic spindles in one-cell C. elegans embryos. *PLoS ONE* **5**, e12301.

Rual, J.-F., Ceron, J., Koreth, J., Hao, T., Nicot, A.-S., Hirozane-Kishikawa, T., Vandenhaute, J., Orkin, S. H., Hill, D. E., van den Heuvel, S. et al. (2004). Toward improving Caenorhabditis elegans phenome mapping with an ORFeome-based RNAi library. *Genome Res.* **14**, 2162-2168.

Squirrell, J. M., Eggers, Z. T., Luedke, N., Saari, B., Grimson, A., Lyons, G. E., Anderson, P. and White, J. G. (2006). CAR-1, a protein that localizes with the mRNA decapping component DCAP-1, is required for cytokinesis and ER organization in Caenorhabditis elegans embryos. *Mol. Biol. Cell* **17**, 336-344.

Srayko, M., Quintin, S., Schwager, A. and Hyman, A. A. (2003). Caenorhabditis elegans TAC-1 and ZYG-9 form a complex that is essential for long astral and spindle microtubules. *Curr. Biol.* **13**, 1506-1511.

Srinivasan, D. G., Fisk, R. M., Xu, H. and van den Heuvel, S. (2003). A complex of LIN-5 and GPR proteins regulates G protein signaling and spindle function in C. elegans. *Genes Dev.* **17**, 1225-1239.

Thyagarajan, K., Afshar, K. and Gönczy, P. (2011). Polarity mediates asymmetric trafficking of the Gbeta heterotrimeric G-protein subunit GPB-1 in C. elegans embryos. *Development* **138**, 2773-2782.

Toyoshima, F. and Nishida, E. (2007). Integrin-mediated adhesion orients the spindle parallel to the substratum in an EB1- and myosin X-dependent manner. *EMBO J.* **26**, 1487-1498.

Tsou, M.-F. B., Hayashi, A. and Rose, L. S. (2003). LET-99 opposes Galpha/GPR signaling to generate asymmetry for spindle positioning in response to PAR and MES-1/SRC-1 signaling. *Development* **130**, 5717-5730.

Velarde, N., Gunsalus, K. C. and Piano, F. (2007). Diverse roles of actin in C. elegans early embryogenesis. *BMC Dev. Biol.* **7**, 142.

Wilbur, J. D., Chen, C.-Y., Manalo, V., Hwang, P. K., Fletterick, R. J. and Brodsky, F. M. (2008). Actin binding by Hip1 (huntingtin-interacting protein 1) and Hip1R (Hip1-related protein) is regulated by clathrin light chain. *J. Biol. Chem.* **283**, 32870-32879.